



Substructure Real-time Hybrid Simulation With a Small-scale Uni-axial Shake Table

R. Zhang¹, P.V. Lauenstein², B.M. Phillips³

*1 Ph.D. Student, Dept. of Civil and Environmental Engineering, University of Maryland, College Park, United States.
E-mail: rzhang15@umd.edu*

*2 Undergraduate Researcher, Dept. of Civil and Environmental Engineering, University of Maryland, College Park,
United States. E-mail: plauen@umd.edu*

*3 Assistant Professor, Dept. of Civil and Environmental Engineering, University of Maryland, College Park, United States.
E-mail: bphilli@umd.edu*

ABSTRACT

Recent investments in earthquake engineering research have produced a vast array of experimental equipment and testing capabilities worldwide. Structural engineering laboratories are often equipped with shake tables, ranging from simple uni-axial tables to six-degree-of-freedom tables to multiple table arrays. These tables are capable of providing the interface boundary conditions necessary for substructure real-time hybrid simulation (RTHS). In the simplest case, the lower stories of a shear building can be simulated numerically while the upper stories tested experimentally. Even this simple case reveals the challenges of RTHS using shake tables. First of all, shake tables are highly nonlinear devices, making modeling and control a challenging task. Furthermore, the mass of the test specimen is typically large relative to the capacity of the table, leading to substantial coupling of the dynamics of the table and specimen. These challenges are exacerbated by RTHS due to the loop of action and reaction between numerical and experimental components. Any delay or lag in the realization of the desired table trajectory and measurement of the base shear can introduce inaccuracies and instabilities into the loop. This research investigates the challenges of RTHS using shake tables through a simple small-scale uni-axial shake table and shear building specimen. A model-based shake table control approach is successfully implemented on a table exhibiting large control-structure interaction and a specimen with low structural damping which leads to sensitivity to delays and lags in the RTHS loop. Results from RTHS and numerical simulations exhibit good agreement. The methods proposed can be extended to more complex specimens through more sophisticated shake table equipment, enabling renewed experimental capabilities with limited additional investments.

KEYWORDS: *Real-time hybrid simulation, shake table testing, shake table control, acceleration tracking.*

1. INTRODUCTION

Real-time hybrid simulation (RTHS) has been increasingly recognized as a powerful experiment technique to evaluate the performance of structural components subjected to ground excitations. Essentially, it is a variation of hybrid simulation in which the structural analysis is executed in real time, thus offering the capability to test rate-dependent components, such as dampers [1-3]. RTHS provides an attractive alternative to traditional shake table testing for earthquake engineering studies [4] by combining experimental testing and numerical simulation in an efficient and cost-effective framework. Structural components for which the response is well understood are modeled numerically, greatly reducing the required laboratory space and equipment. Because only the less understood, critical structural components are physically tested, they can be large or full-scale representations of the actual components, reducing size effects. In this way, even small laboratories can conduct accurate experiments of complex structures. The loop of action and reaction between experimental and numerical components is carried out in real-time, ensuring accurate representation of both the local and global dynamic behavior of the structure.

One of the challenges for RTHS is that it requires a fixed, small sampling time (typically, less than 10 ms) in execution of each testing cycle. Moreover, unless properly compensated, time delays and time lags introduced by the experimental equipment are likely to lead to stability and accuracy problems [5]. One of the most effective approaches to mitigate the effect of time delays and time lags is through actuator control strategies designed to compensate for the modeled dynamics of the servo-hydraulic system [6, 7].

Shake tables present an opportunity in the area of RTHS because the equipment is widely available and the creation of substructure boundary conditions is straightforward. The shake table base plate can serve as the interface between numerical and experimental substructures, a convenient convention for certain structural systems. For example, uniaxial and biaxial shake tables can provide boundary conditions mid-height for shear type structures. More complex shake tables, such as six-degree-of-freedom (6DOF) tables, can provide complex boundary conditions mid-height for tall structures that undergo complex three-dimensional translations and rotations.

Unlike traditional shake table testing, with RTHS the accelerations to be tracked are not known prior to testing. Therefore, shake table control strategies in the literature requiring offline calculations and configuration (e.g., [8-10]) cannot be used for real-time testing where the acceleration is calculated online from the numerical integration. In contrast, some recently developed acceleration-tracking shake table control strategies (e.g., [11, 12, 13]) do not require the desired acceleration to be predefined and can potentially be employed in RTHS. In this study a model-based control strategy consisting of both feedforward and feedback links is selected to provide the required real-time acceleration control [13].

2. RTHS USING A SHAKE TABLE

For a simple illustration of the use of a shake table in RTHS, a linear 3DOF shear building is considered (see Fig. 2.1(a)). The equations of motion governing the dynamic response of the structure subjected to an input ground motion are represented as follows:

$$\begin{bmatrix} m_1 & 0 & 0 \\ 0 & m_2 & 0 \\ 0 & 0 & m_3 \end{bmatrix} \begin{Bmatrix} \ddot{x}_1 \\ \ddot{x}_2 \\ \ddot{x}_3 \end{Bmatrix} + \begin{bmatrix} c_1 + c_2 & -c_2 & 0 \\ -c_2 & c_2 + c_3 & -c_3 \\ 0 & -c_3 & c_3 \end{bmatrix} \begin{Bmatrix} \dot{x}_1 \\ \dot{x}_2 \\ \dot{x}_3 \end{Bmatrix} + \begin{bmatrix} k_1 + k_2 & -k_2 & 0 \\ -k_2 & k_2 + k_3 & -k_3 \\ 0 & -k_3 & k_3 \end{bmatrix} \begin{Bmatrix} x_1 \\ x_2 \\ x_3 \end{Bmatrix} = - \begin{bmatrix} m_1 & 0 & 0 \\ 0 & m_2 & 0 \\ 0 & 0 & m_3 \end{bmatrix} \begin{Bmatrix} 1 \\ 1 \\ 1 \end{Bmatrix} \ddot{x}_g \quad (2.1)$$

where m_i , c_i , and k_i are the mass, damping, and stiffness of the i -th story, x_i is displacement relative to the ground of the i -th story, \ddot{x}_g is the ground acceleration, and dots represent differentiation with respect to time. For RTHS, the equations of motion in Eq. 2.1 are separated into numerical and experimental components as in Eq. 2.2 and Fig. 2.1(b). Structural parameters as well as DOF associated with the experimental substructure are indicated by the superscript “E”. Structural parameters as well as DOF associated with the numerical substructure are indicated by the superscript “N”. The DOF at the interface between components are indicated by the superscript “I”.

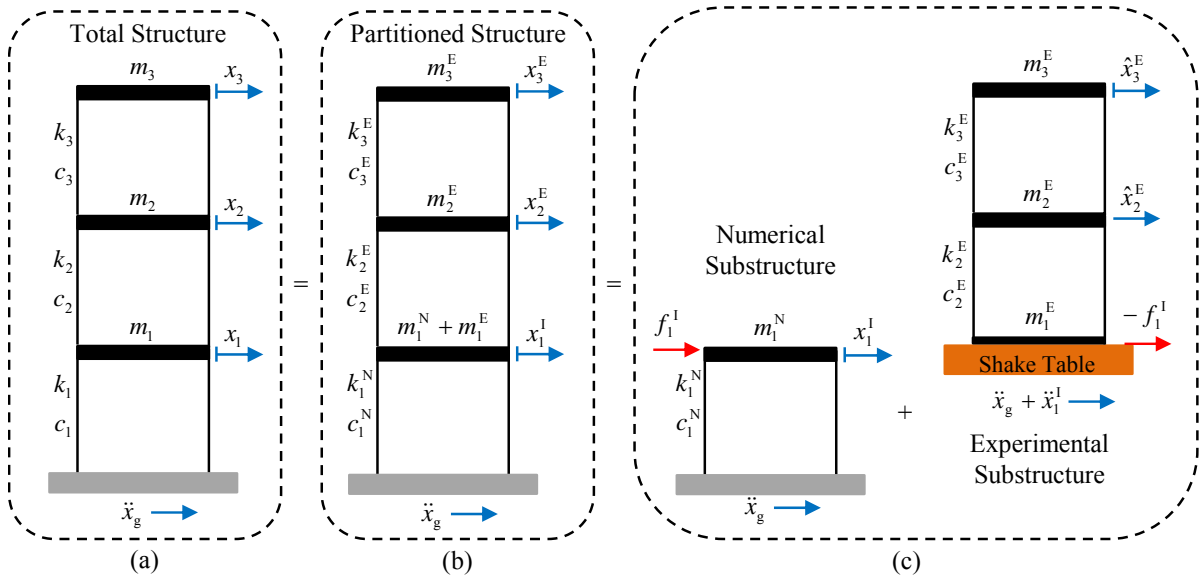


Figure 2.1 Example 3DOF structure for RTHS using a shake table

$$\begin{bmatrix} m_1^N + m_1^E & 0 & 0 \\ 0 & m_2^E & 0 \\ 0 & 0 & m_3^E \end{bmatrix} \begin{Bmatrix} \ddot{x}_1^I \\ \ddot{x}_2^E \\ \ddot{x}_3^E \end{Bmatrix} + \begin{bmatrix} c_1^N + c_2^E & -c_2^E & 0 \\ -c_2^E & c_2^E + c_3^E & -c_3^E \\ 0 & -c_3^E & c_3^E \end{bmatrix} \begin{Bmatrix} \dot{x}_1^I \\ \dot{x}_2^E \\ \dot{x}_3^E \end{Bmatrix} + \begin{bmatrix} k_1^N + k_2^E & -k_2^E & 0 \\ -k_2^E & k_2^E + k_3^E & -k_3^E \\ 0 & -k_3^E & k_3^E \end{bmatrix} \begin{Bmatrix} x_1^I \\ x_2^E \\ x_3^E \end{Bmatrix} = \begin{bmatrix} m_1^N + m_1^E & 0 & 0 \\ 0 & m_2^E & 0 \\ 0 & 0 & m_3^E \end{bmatrix} \begin{Bmatrix} 1 \\ 1 \\ 1 \end{Bmatrix} \ddot{x}_g \quad (2.2)$$

Numerical integration is performed solely on the numerical substructure, containing both numerical and interface DOF. This approach is consistent with the dynamic substructuring approach of Shing [14]. The numerical substructure is described by the following equations of motion:

$$m_1^N \ddot{x}_1^I + c_1^N \dot{x}_1^I + k_1^N x_1^I = -m_1^N \ddot{x}_g + f_1^I \quad (2.3)$$

The contribution from the experimental substructure is included as an external force f_1^I . The experimental substructure follows the equations of motion:

$$\begin{bmatrix} m_1^E & 0 & 0 \\ 0 & m_2^E & 0 \\ 0 & 0 & m_3^E \end{bmatrix} \begin{Bmatrix} \ddot{x}_1^I \\ \ddot{x}_2^E \\ \ddot{x}_3^E \end{Bmatrix} + \begin{bmatrix} c_2^E & -c_2^E & 0 \\ -c_2^E & c_2^E + c_3^E & -c_3^E \\ 0 & -c_3^E & c_3^E \end{bmatrix} \begin{Bmatrix} \dot{x}_1^I \\ \dot{x}_2^E \\ \dot{x}_3^E \end{Bmatrix} + \begin{bmatrix} k_2^E & -k_2^E & 0 \\ -k_2^E & k_2^E + k_3^E & -k_3^E \\ 0 & -k_3^E & k_3^E \end{bmatrix} \begin{Bmatrix} x_1^I \\ x_2^E \\ x_3^E \end{Bmatrix} = \begin{bmatrix} m_1^E & 0 & 0 \\ 0 & m_2^E & 0 \\ 0 & 0 & m_3^E \end{bmatrix} \begin{Bmatrix} 1 \\ 1 \\ 1 \end{Bmatrix} \ddot{x}_g - \begin{Bmatrix} f_1^I \\ 0 \\ 0 \end{Bmatrix} \quad (2.4)$$

Toward creating an experimental substructure appropriate for shake table testing, the DOF of Eq. 2.4 can be redefined relative to the interface DOF. Taking $\hat{x}_2^E = x_2^E - x_1^I$ and $\hat{x}_3^E = x_3^E - x_1^I$, Eq. 2.4 can be separated into equations of motion for the experimental substructure relative to the base of the shake table, subject to a base acceleration:

$$\begin{bmatrix} m_2^E & 0 \\ 0 & m_3^E \end{bmatrix} \begin{Bmatrix} \ddot{\hat{x}}_2^E \\ \ddot{\hat{x}}_3^E \end{Bmatrix} + \begin{bmatrix} c_2^E + c_3^E & -c_3^E \\ -c_3^E & c_3^E \end{bmatrix} \begin{Bmatrix} \dot{\hat{x}}_2^E \\ \dot{\hat{x}}_3^E \end{Bmatrix} + \begin{bmatrix} k_3^E & -k_3^E \\ -k_3^E & k_3^E \end{bmatrix} \begin{Bmatrix} \hat{x}_2^E \\ \hat{x}_3^E \end{Bmatrix} = - \begin{bmatrix} m_2^E & 0 \\ 0 & m_3^E \end{bmatrix} \begin{Bmatrix} 1 \\ 1 \end{Bmatrix} \ddot{x}_{1,abs}^I \quad (2.5)$$

and the base shear, or external force to return to the numerical substructure:

$$f_1^I = -m_1^E \ddot{x}_{1,abs}^I - m_2^E \ddot{\hat{x}}_{2,abs}^E - m_3^E \ddot{\hat{x}}_{3,abs}^E \quad (2.6)$$

where $\ddot{x}_{1,abs}^I = \ddot{x}_1^I + \ddot{x}_g$, $\ddot{\hat{x}}_{2,abs}^E = \ddot{\hat{x}}_2^E + \ddot{x}_{1,abs}^I$, and $\ddot{\hat{x}}_{3,abs}^E = \ddot{\hat{x}}_3^E + \ddot{x}_{1,abs}^I$. The numerical and experimental substructures are illustrated in Fig. 2.1(c). The procedure for RTHS using a shake table in this configuration can be extracted from Eq. 2.3, Eq. 2.5, and Eq. 2.6. Fig. 2.2 illustrates a block diagram of RTHS with shake table control. To summarize, the numerical substructure is excited by ground acceleration and the numerical and interface DOF values are determined through numerical integration. The absolute acceleration of the interface DOF is taken as the desired acceleration for the shake table. This acceleration is not known prior to testing, requiring a special class of shake table control strategies that can track accelerations determined online. The base shear due to the mass, damping, and stiffness of the specimen must be measured and returned to the numerical substructure. Here, it is important to include only the dynamics of the structure and not that of the shake table (e.g., the shake table mass). This loop of action and reaction is carried out in real time until the entire response history has been conducted.

3. SHAKE TABLE CONTROL FOR RTHS

To capture the inertial effects of the experimental substructure, the shake table must be able to track the desired accelerations accurately (e.g., absolute acceleration at the interface between numerical and experimental substructures). Without compensation, the dynamics of the shake table appear within the RTHS loop. Phase lags from command to response of the shake table as well as the dynamic coupling between the shake table and the specimen have a direct impact on the accuracy and stability of the RTHS loop. The model-based shake table control strategy used in this study is based on a linearized model of the shake table system [13]. The goal of this strategy is to cancel out the modeled dynamics of the shake table through feedforward control and provide robustness to changes in specimen dynamics (e.g., damage) and to shake table nonlinearities and uncertainties (e.g., friction and modeling errors) through feedback control.

The first step to implement the model-based control is to represent the shake table system as a linearized transfer function from input voltage command u to output measured acceleration a_m . The model parameters are determined using system identification. Fig. 4.1(a) shows the experimentally identified transfer function of the shake table using a 10 Hz band-limited white noise with an 2DOF experimental specimen mounted on the table. Two features can be clearly seen from this figure. First, since the command to the shake table is approximately proportional to the displacement, the output acceleration approaches zero at zero frequency. Second, there are valleys around the two natural frequencies of the experimental specimen, clearly illustrating the interaction between shake table and specimen (i.e., control-structure interaction; CSI). In all, 8 poles and 8 zeros are used to create a model (shown in Fig. 4.1(a)) that matches the experimentally identified transfer function.

The feedforward controller (FF) is created as an inverse of the identified model. The inverse is proper and stable, requiring no modification. The feedback controller (FB) is created using LQG control to minimize the error between the desired and measured accelerations. More information on the model-based shake table control strategy can be found in [13]. The shake table control strategy in the context of RTHS is illustrated in Fig. 2.2.

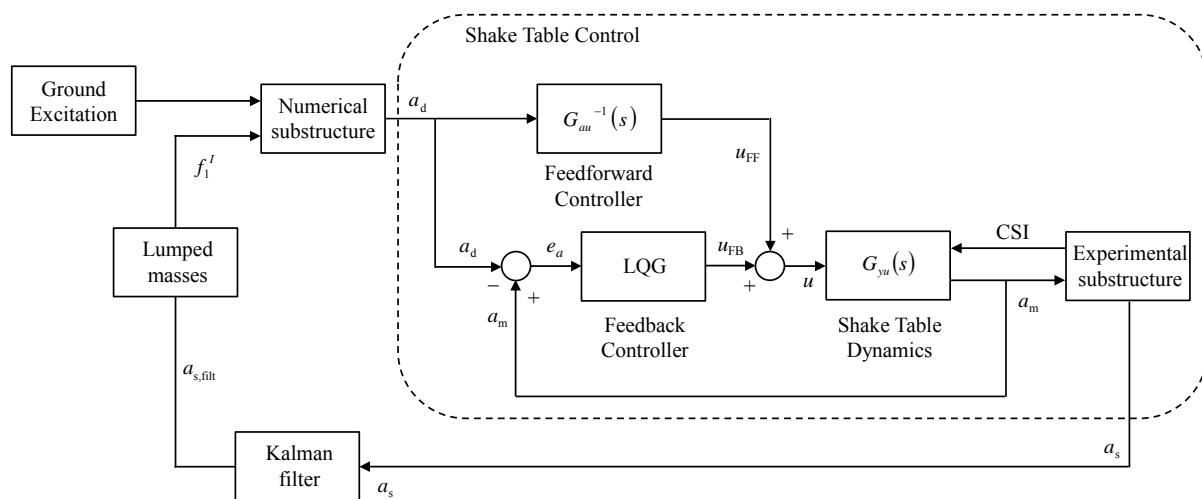


Figure 2.2 Block diagram of shake table RTHS including model-based controller

4. EXPERIMENTAL SETUP

The substructure RTHS procedure is developed and verified using a small-scale uni-axial shake table as shown in Fig. 4.1(b). The setup consists of a uni-axial shake table, a two-story steel shear building model as the experimental specimen/substructure, and a control and data acquisition system. The dynamic properties of both the experimental substructure and the total structure are presented in this section. The equipment is located at the University of Maryland and is part of the Structural Engineering Laboratory.

4.1 Uni-axial Shake Table

The shake table used in this study is a model APS 400 ELECTRO-SEIS manufactured by SPEKTRA. It has a $35.6 \text{ cm} \times 35.6 \text{ cm}$ top plate driven by an electrodynamic vibration generator with a stroke of $\pm 15.8 \text{ cm}$. The shake table has a dynamic load capacity of 445 N and it can support a payload up to 23 kg.

The control hardware for the shake table consists of a dSPACE DS1103 Controller Board and a windows-based host PC. The controller board, working as a real-time controller, is fully programmable from the MATLAB Simulink block diagram environment. The sensors and data acquisition system includes a dSPACE 16-bit high-speed multifunction data acquisition board with 8 D/A channels and 20 A/D channels, a 4-channel PCB Piezotronics signal conditioner (Model 4821C), and four PCB Piezotronics accelerometers (Model 393B04). The accelerometers attached on both shake table and the testing structure have a measurement range of $\pm 5 \text{ g}$, a frequency range of 0.05 to 750 Hz, and a sensitivity of 1000 mV/g.

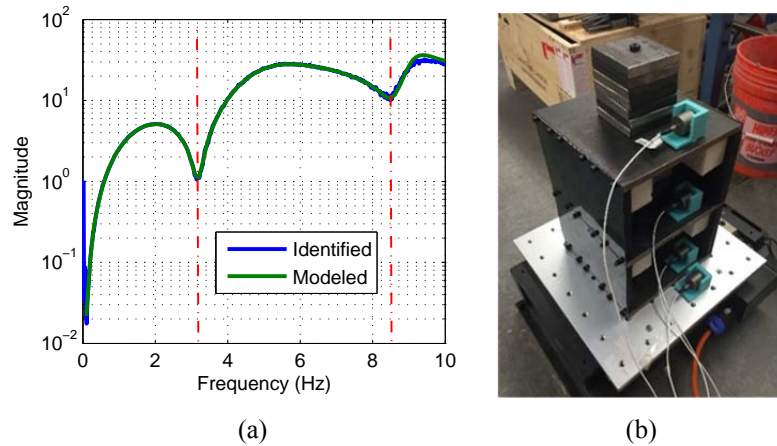


Figure 4.1 Shake table with experimental substructure: (a) input-output transfer function; (b) laboratory view

4.2 Experimental Substructure

A two-story steel shear building model is used as the experimental specimen/substructure as shown in Fig. 4.1(b). The floor size is $20.3 \text{ cm} \times 20.3 \text{ cm}$ and the height of each story is 14.0 cm . At each floor, seven steel blocks are attached as additional masses. The total mass of the first and second floor is 6.91 kg and 6.95 kg , respectively. Two spring-steel columns with a thickness of 0.5 mm connect the floor plates. The spring steel ensures that the building can undergo large deformations without yielding. Foam is added to the connections between the columns and floor plates to increase the structural damping. Inherent structural damping is directly tied to the stability of the RTHS and lightly damped structures are especially challenging to control. In this case, the bare steel structure exhibited very small damping, approximately 0.5% for the 1st mode. The added foam damping reduced stability concerns for this simple study, and can be removed in future studies. The specimen properties were identified using a 0 to 10 Hz band-limited white noise base excitation. The natural frequencies were identified to be 3.2 Hz and 8.4 Hz with corresponding damping ratios of 4.3% and 3.9% determined using free vibration tests.

4.3 Total Structure

The total three-story shear structure consists of a numerically simulated lower story and experimentally represented upper stories. The mass and stiffness of the lower story are chosen as the average of the mass and stiffness of the upper two stories, resulting in natural frequencies of 2.3 Hz , 6.5 Hz , and 9.2 Hz . To analyze the damping influence on the performance of RTHS, two values of damping are chosen for the numerical first story which result in damping ratios of either 2.6% or 3.6% for the 1st mode of the total structure. Natural frequencies and damping ratios of the total structure are designed to be similar to those of typical midrise steel structure [15].

4.4 Earthquake Ground Motions

Two earthquake ground motion records with different magnitudes and frequency content are selected as the input to the structure [16]: (1) El Centro: The N-S component recorded at the Imperial Valley Irrigation District substation in El Centro, California, during the Imperial Valley, California earthquake of May 18, 1940, and (2) Hachinohe: The N-S component recorded at Hachinohe City during the Tokachi-oki earthquake of May 16, 1968. The reference earthquakes are passed through a 2-pole Butterworth high-pass filter with a cutoff frequency of 0.25 Hz to remove the very low-frequency behavior without altering the desired frequency content. Note that all earthquake records are scaled to 30% of the original amplitude due to the stroke limitation of the shake table.

5. PERFORMANCE OF SHAKE TABLE CONTROL AND EXPERIMENTAL RESULTS

This section investigates the performance of the proposed RTHS techniques with a focus on tracking the desired acceleration signal and achieving overall accurate RTHS when compared to numerical simulations. First, acceleration tracking performance of feedforward control (FF) and combined feedforward-feedback (FF + FB) control are presented for both predefined accelerations and accelerations determined online during RTHS.

Second, an approach to avoid high-frequency oscillations in the RTHS loop due to measurement noise is presented. Third, RTHS results are compared to numerical simulations to verify the overall performance of the proposed RTHS techniques. The results and conclusions are based on the lower damping case (2.6% in the 1st mode) with FF + FB control strategy unless otherwise explicitly stated.

5.1 Acceleration Tracking

The acceleration tracking performance for the FF + FB controller is shown in Fig. 5.1 at the shake table level for two cases excited by the 30% El Centro record: (1) traditional shake table test on the experimental specimen alone and (2) RTHS of the 3DOF structure where the shake table is tracking the interface between numerical and experimental substructures. Good tracking performance is observed regardless of whether the acceleration is determined online or offline. Quantitative tracking results are summarized in Table 5.1 including those for the FF controller alone. Because the shake table and specimen are accurately described by a linear model and the specimen doesn't exhibit damage, feedforward control alone provides excellent tracking. The tracking performance is enhanced by feedback control, improving robustness to modeling errors and nonlinearities.

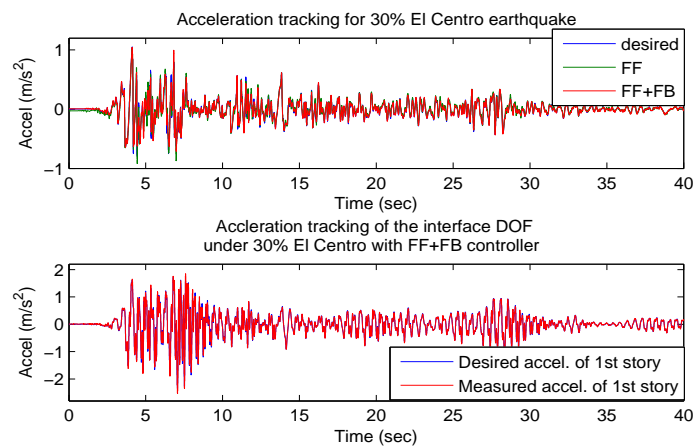


Figure 5.1 Acceleration tracking performance for traditional shake table testing (top) and RTHS (bottom)

5.2 Filtering of Measured Accelerations

In RTHS, measurement noise from sensors can enter into the numerical substructure and result in high-frequency commands to the experimental substructure. High-frequency content in the RTHS loop could lead to problems for numerical integration stability or damage to the experimental equipment. As shown in Eq. 2.6, noise in the acceleration measurements may induce undesired behavior of the shake table. To eliminate this phenomenon, a Kalman filter is added. The Kalman filter takes inputs of measured acceleration from the experimental DOF and uses the identified model of the experimental specimen to estimate a cleaner signal. Uncertainties are assumed to enter the model in the same way as the input ground motion. The parameters of Kalman filter for this study are determined as $Q=1 \times 10^3$, $R=I_{2 \times 2}$. Fig. 5.2 shows the acceleration before and after filtering of the top floor of the experimental substructure when the total structure is subjected to 30% El Centro through RTHS. From the zoomed-in view, it is observed that the noise contained in the measured accelerations is eliminated by the Kalman filter without altering the dominant structural responses. Most importantly, the Kalman filter does not introduce phase lag which would lead to stability problems in the RTHS loop.

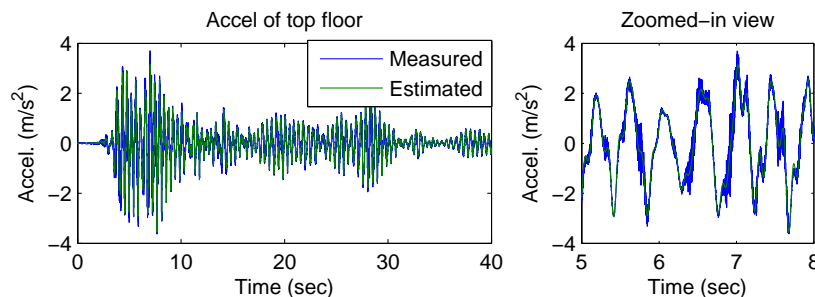


Figure 5.2 Effect of Kalman filter on acceleration measurements

Table 5.1 Acceleration tracking performance for (1) traditional shake table test, and (2) RTHS

Controller	(1) Traditional shake table test		(2) RTHS of the 3-story structure	
	Max tracking error (m/s ²)	RMS tracking error (m/s ²)	Max tracking error (m/s ²)	RMS tracking error (m/s ²)
FF	0.0376	0.0030	0.1007	0.0058
FF + FB	0.0086	0.0004	0.1922	0.0027

5.3 Performance of RTHS

In this section, the performance of RTHS is presented for the two structures with different damping ratios subjected to 30% El Centro and 30% Hachinohe records. The experimental results are compared to numerical simulation results. All cases are listed as below:

1. Numerical simulation of the total 3-story structure (SIM);
2. Numerical simulation of the total 3-story structure, substructured into two numerical substructures with a 5 ms delay passing the base shear from the upper two stories to lower story (SIM-DELAY); and
3. RTHS of the 3-story structure (EXP-RTHS).

Table 5.2 summarizes the overall RTHS performance of absolute accelerations for the two structure systems with different damping ratios subjected to 30% El Centro and 30% Hachinohe records. The RMS tracking errors of both SIM-DELAY and EXP-RTHS are calculated by comparing their respective results to the numerical simulation case SIM. From Table 5.2, it is observed that the RMS tracking errors of EXP-RTHS are small which indicates good RTHS performance. EXP-RTHS results are better than the illustrative reference case SIM-DELAY, which is nearly identical to the SIM case, except for the small 5 ms delay between substructures. As expected, better RTHS performance is demonstrated for structure with larger damping. Fig. 5.3 shows the time histories of the absolute accelerations for the low damping structure subjected to 30% Hachinohe. The RTHS techniques perform well not only on the peak responses but also throughout the entire time history.

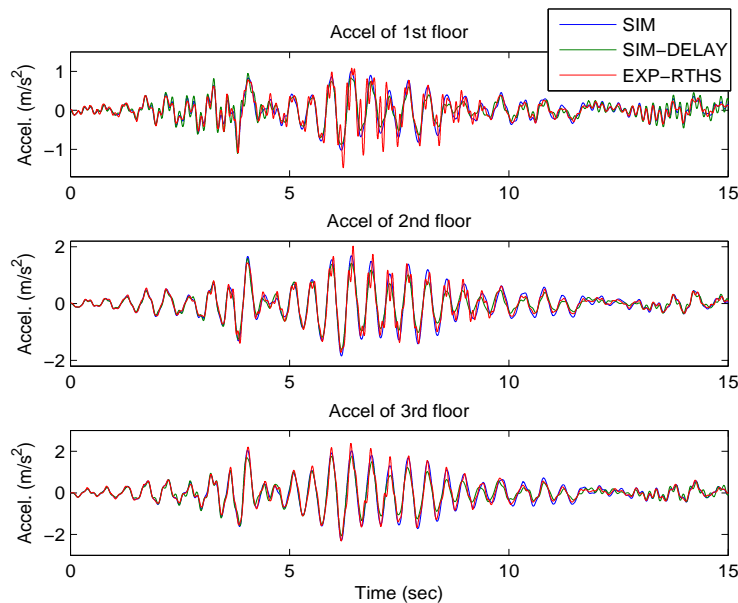


Figure 5.3 Performance of RTHS compared to numerical simulations

Table 5.2 RTHS performance of absolute accelerations for structures with different damping ratios

Earthquake excitation	Story	RMS tracking error (m/s ²)			
		Structure with lower damping		Structure with higher damping	
		SIM-DELAY	EXP-RTHS	SIM-DELAY	EXP-RTHS
30% El Centro	1 st	0.0236	0.0158	0.0297	0.0023
	2 nd	0.1050	0.0466	0.0759	0.0428
	3 rd	0.1228	0.0615	0.0913	0.0500
30% Hachinohe	1 st	0.0167	0.0016	0.0172	0.0003
	2 nd	0.0617	0.0201	0.0439	0.0145
	3 rd	0.0733	0.0179	0.0532	0.0095

6. CONCLUSIONS AND RECOMMENDATIONS

This study investigated the RTHS technique using a uni-axial shake table with a model-based shake table control strategy. Shake tables provide an excellent tool for RTHS studies due to their widespread availability and ease of creating and enforcing interface boundary conditions between numerical and experimental substructures. A simple formulation for RTHS using shake tables has been presented. Essentially, the shake table must track the absolute acceleration of the interface DOF, requiring advanced online shake table control strategies. Modeled dynamics of the shake table, including the substantial coupling with the specimen, were used to develop feedforward and feedback controllers for the model-based control approach. Furthermore, a Kalman filter was included to reduce high-frequency noise in the measured accelerations fed back to the numerical substructure.

The proposed strategy for shake table control in the context of RTHS has been verified to offer a good online acceleration tracking performance. The Kalman filter adequately removed high-frequency sensor noise to avoid high-frequency commands to the shake table while also avoiding introducing phase lag associated with many filters that could lead to RTHS instability. The effectiveness of proposed techniques was verified through a series of RTHS using a uni-axial shake table and two-story steel frame structure at the University of Maryland. The results from RTHS and numerical simulations exhibit good agreement for the simple linear structure.

Future studies will expand the technique beyond proof-of-concept studies.

REFERENCES

1. Carrion, J. E., Spencer Jr., B. F., and Phillips, B. M. (2009). "Real-time hybrid simulation for structural control performance assessment." *Earthquake Engineering and Engineering Vibration*, 8(4), 481-492.
2. Christenson, R. E., Lin, Y. Z., Emmons, A., and Bass, B. (2008). "Large-scale experimental verification of semiactive control through real-time hybrid simulation." *Journal of Structural Engineering*, 134(4), 522-534.
3. Zapateiro, M., Karimi, H., Luo, N., and Spencer Jr., B. F. (2010). "Real-time hybrid testing of semiactive control strategies for vibration reduction in a structure with MR damper." *Structural Control and Health Monitoring*, 17(4), 427-451.
4. Nakashima, M., Kato, H., and Takaoka, E. (1992). "Development of real-time pseudo dynamic testing." *Earthquake Engineering & Structural Dynamics*, 21(1), 79-92.
5. Horiuchi, T., Nakagawa, M., Sugano, M., and Konno, T. (1996). "Development of a real-time hybrid experimental system with actuator delay compensation." *Proc., 11th World Conference Earthquake Engineering*.
6. Carrion, J. E. and Spencer Jr., B. F. (2007). "Model-based strategies for real-time hybrid testing." *NSEL Report Series*, University of Illinois.
7. Phillips, B. M. and Spencer Jr., B. F. (2012). "Model-based feedforward-feedback actuator control for real-time hybrid simulation." *Journal of Structural Engineering*, 139(7), 1205-1214.
8. Fletcher, J. N. (1990). "Global simulation: new technique for multi-axis test control." *Sound and Vibration*, 24(11), 26-33.
9. Simova, M., and Mamucevski, D. (1980). "On-line control of single component shaking table." *Proc., 7th World Conference on Earthquake Engineering*, 63-69.
10. Spencer Jr., B. F., and Yang, G. (1998). "Earthquake simulator control by transfer function iteration." *Proc., Proc., 12th ASCE Engineering Mechanics Conference*, 17-20.
11. Kuehn, J., Epp, D., and Patten, W. (1999). "High-fidelity control of a seismic shake table." *Earthquake Engineering & Structural Dynamics*, 28(11), 1235-1254.
12. Nakata, N. (2011). "A multi-purpose earthquake simulator and a flexible development platform for actuator controller design." *Journal of Vibration and Control*, 1077546311421946.
13. Phillips, B. M., Wierschem, N. E., and Spencer, B. (2014). "Model-based multi-metric control of uniaxial shake tables." *Earthquake Engineering & Structural Dynamics*, 43(5), 681-699.
14. Shing, P. B. (2008). "Real-time hybrid testing techniques." *Modern Testing Techniques for Structural Systems*, Springer, 259-292.
15. ASCE, (2010). *Minimum Design Loads for Buildings and Other Structures*, American Society of Civil Engineers, Structural Engineering Institute, Reston, V.A.
16. Ohtori, Y., Christenson, R. E., Spencer Jr., B. F., and Dyke, S. J. (2004). "Benchmark control problems for seismically excited nonlinear buildings." *Journal of Engineering Mechanics*, 130(4), 366-385.